Combination Therapy with the Advanced Glycation End Product Cross-Link Breaker, Alagebrium, and Angiotensin Converting Enzyme Inhibitors in Diabetes: Synergy or Redundancy?

Melinda T. Coughlan, Vicki Thallas-Bonke, Josefa Pete, David M. Long, Anna Gasser, David C. K. Tong, Maryann Arnstein, Suzanne R. Thorpe, Mark E. Cooper, and Josephine M. Forbes

Albert Einstein Juvenile Diabetes Research Foundation Centre for Diabetes Complications (M.T.C., V.T.-B., J.P., D.M.L., A.G., D.C.K.T., M.A., M.E.C., J.M.F.), Wynn Domain, Baker Medical Research Institute, Melbourne, Victoria 8008, Australia; Department of Chemistry and Biochemistry (S.R.T.), University of South Carolina, Columbia, South Carolina 29208; and Department of Immunology (M.E.C., J.M.F.), Monash University, Alfred Medical Research and Education Precinct, Melbourne, Victoria 3004, Australia

Blockade of advanced glycation end product (AGE) accumulation with alagebrium with concomitant angiotensin converting enzyme inhibition was tested for effects on renal function and on other postulated mediators of diabetic renal disease including the renin-angiotensin system, AGEs, mitochondrial and cytosolic oxidative stress, and intracellular signaling molecules. Sprague Dawley rats were rendered diabetic with streptozotocin and followed consecutively for 32 wk with nondiabetic controls. Groups were treated with ramipril (1 mg/kg·d; wk 0–32); alagebrium (10 mg/kg·d; wk 16–32); or a combination of both. Although individual treatments had significant effects on albuminuria, no further improvements were seen with combination therapy. Changes in urinary vascular endothelial growth factor excretion mirrored those seen in albuminuria. Diabetes was associated with suppression of circulating angiotensin II in the context of increased circulating and renal levels of the AGE, carboxymethyllysine. All treatments attenuated circulating but not renal carboxymethyllysine levels. The renal gene expression of AGE receptor 1 and soluble receptor for advanced glycation end products were markedly reduced by diabetes and normalized with alagebrium. Diabetes induced renal mitochondrial oxidative stress, which was reduced with alagebrium. In the cytosol, both therapies were equally effective in reducing reactive oxygen species production. Increases in membranous protein kinase C activity in diabetes were attenuated by all treatments, whereas diabetes-associated increases in nuclear factor-κB p65 translocation remained unaltered by any therapy. It is evident that renin-angiotensin system blockade and AGE inhibition have specific effects. However, many of their downstream effects appear to be similar, suggesting that their renoprotective benefits may ultimately involve common pathways and key points of convergence, which could be important targets for new therapies in diabetic nephropathy. (*Endocrinology* 148: 886–895, 2007)

D IABETIC RENAL DISEASE appears to occur as the result of an interplay between hemodynamic and metabolic factors (1, 2). Approaches which focus on attenuating the intrarenal hemodynamic abnormalities associated with diabetes such as agents that interrupt the renin-angiotensin system (RAS), namely angiotensin converting enzyme-1 (ACEi) inhibitors (3) and angiotensin II (Ang II) receptor antagonists (4), respectively, are currently the most effective clinical interventions for the prevention and treatment of diabetic nephropathy, as assessed by urinary albumin excretion. Other known hypotensive agents without effects on the RAS do not confer the same degree of renoprotection in diabetic complications (5), implying that the nonhemodynamic mechanisms seen with RAS blockade, may be equally important contributors to their protective actions. Although poorly characterized in the diabetic context, these potentially downstream pathways are thought to include oxidative stress with both mitochondrial and cytosolic sources of reactive oxygen species (ROS) implicated in a range of diabetic vascular complications (6–8). Various intracellular signaling pathways involved in diabetic complications and known to be activated by Ang II such as nuclear factor-κB (NF-κB) and protein kinase C (PKC) (9–11) could potentially be inhibited in diabetic complications *in vivo* via interruption of the RAS, although this has not been specifically examined.

Another pathway implicated in the pathogenesis and progression of diabetic complications is the biochemical process of advanced glycation (12). In diabetes, primarily as a result of chronic hyperglycemia, there is an accumulation of advanced glycation end products (AGEs), particularly in the kidney (13). One of the major ways that AGEs induce end-organ injury is via a ligand-receptor interaction with the Ig-like protein, receptor for AGEs (RAGE), which is widely expressed in the kidney including in podocytes (14) and

tubular epithelial cells (15). In a range of *in vitro* studies, including in various renal cell populations, AGEs promote cytosolic oxidative stress and expression of various growth factors including vascular endothelial growth factor (VEGF), primarily via RAGE (14). These effects on VEGF expression are particularly relevant to the pathogenesis of diabetes-associated albuminuria with various studies using both VEGF receptor antagonists or neutralizing antibodies to VEGF having been recently reported to attenuate urinary albumin excretion in experimental diabetes (16–18). Furthermore, these AGEs may activate other intracellular signaling molecules such as NF-κB (19).

Finally, the identification and characterization of direct interactions, as assessed both *in vitro* and *in vivo* (20), between AGEs and the RAS (21, 22) provides the rationale to further determine key downstream events in both pathways, which may explain the renoprotective effects conferred by agents that either attenuate renal AGE accumulation or interrupt the intrarenal RAS. Thus, in the present study, the *in vivo* effects of the ACEi, ramipril, and the AGE cross-link breaker, alagebrium, as well as the combination of these agents was examined in a model of experimental diabetes with a particular focus on the major pathways affected by these agents, specifically the intrarenal RAS and advanced glycation. Furthermore, possible downstream pathways influenced by both AGEs and AngII and known to be activated in the diabetic kidney were assessed including mitochondrial and cytosolic oxidative stress, PKC and NF-κB. These experiments were thus able to characterize *in vivo* not only the key links among the various pathogenic pathways in the diabetic kidney but also the potential redundancy and synergy between the RAS and advanced glycation pathways.

Materials and Methods

Experimental animal model

Animals were housed in groups of three rats per cage with a 12-h light, 12-h dark cycle and *ad libitum* access to food and water. Experimental diabetes was induced in male Sprague Dawley rats (200–250 g) by iv injection of streptozocin [50 mg/kg, sodium citrate buffer (pH 4.5)] after an overnight fast. Animals with plasma glucose concentrations in excess of 15 mmol/liter, 1 wk after induction of diabetes, were included in the study. Sham injected control animals were followed up concurrently. Diabetic and control animals were randomized into groups (n = 10) that received: 1) no treatment (D and C), 2) the ACE inhibitor ramipril from wk 0 to 32 (CRam, DRam, 1 mg/kg in drinking water; kind gift of Sanofi-Aventis, Bridgewater, NJ), 3) the AGE cross-link breaker alagebrium, (10 mg/kg oral gavage; ALT-711; 4,5-dimethyl-3-(2-oxo2-phenylethyl)-thiazolium chloride, kind gift of Alteon Inc., Ramsey, NJ) as an intervention from wk 16 to 32 (DAlt); or 4) their combination (CRamAlt; DRamAlt), specifically as with the monotherapy group, ramipril from wk 0 and alagebrium from wk 16. The rationale behind commencing intervention with an AGE cross-link breaker was to investigate the efficacy of adjunct therapy with already established ACE inhibition. Two to three units of insulin (Humalog; Eli Lilly, Indianapolis, IN) were administered daily to diabetic animals to prevent ketoacidosis and improve survival. Body weight, mean systolic blood pressure by tail cuff plethysmography (23), glomerular filtration rate using ^{99}Tc-diethylene-triamine pentaacetic acid (24), albumin excretion rate by ELISA (Bethyl Laboratories, Montgomery, TX), and glycated hemoglobin (25) were measured every 8 wk. All animal procedures were in accordance with guidelines set by the Alfred Medical Research and Education Precinct Ethics Committee and the National Health and Medical Research Council of Australia.

Renal fractionation for assays

Two hundred milligrams of renal cortex were homogenized in modified Kreb's buffer [20 mM HEPES (pH 7.2), 1 mM EGTA, 210 mM mannitol, and 70 mM sucrose]. Samples were centrifuged 1500 × *g* for 5 min, supernatant was removed for cytosolic and mitochondrial separation, and the pellet extracted as outlined below for NF-κB determination. The supernatant was centrifuged at 12000 × *g* for 15 min and the subsequent supernatant stored as the cytosolic fraction. The pellet was resuspended in modified Kreb's buffer as the mitochondrial enriched fraction. Total protein was determined by the Bicinchoninic acid method (Pierce, Rockford, IL) according to the manufacturer's instructions.

Carboxymethyllysine (CML) ELISA

CML concentrations in serum, renal mitochondrial, and cytosolic extracts were assessed by indirect ELISA. A seven-point standard curve ranging from 2 to 134 nmol/mol lysine was constructed using AGE-BSA with a known CML content. Sample (diluted 1:10,000 to 1:20,000 for serum; and 1:1,000 for kidney cytosolic and mitochondrial extracts) or standard were diluted in 50 mM carbonate buffer (pH 9.6), and 100 μl were added to a microtiter plate (Nunc-Immuno MaxiSorp; Nunc, Kamstrup, Roskilde, Denmark) and incubated overnight at 4 C. After washing, wells were blocked for 1 h in 1% BSA (Sigma, St. Louis, MO), washed three times, and then 100 μl of a rabbit polyclonal anti-CML antibody (5 μg/ml, described in Ref. 26) was added to each well. After 2 h wells were washed three times, and 100 μl of 0.2 μg/ml goat-antirabbit IgG biotinylated antibody (Dako Corp., Carpinteria, CA) were added to each well. Finally, 100 μl of streptavidin horseradish peroxidase (Dako Corp.), diluted 1/5000, were added. After 30 min, the wells were developed with 100 μl of 3,3′, 5, 5′-tetramethyl benzidine substrate (Sigma), and the reaction was terminated after 15 min with 1.8 M H_2SO_4. The absorbance was quantitated using a microtiter plate reader at 450 nm (Victor 3V; PerkinElmer, Foster City, CA). The limit of detection of the assay was 8.0 nmol/mol lysine. The interassay coefficient of variation was 7.3%. The intraassay coefficient of variation was 5.5%. The linearity of dilution of the assay was $r^2 = 0.91$. Results are expressed in nanomoles per mole lysine per milligram protein as determined in the standard by selected ion monitoring gas chromatography-mass spectrometry (27).

Urinary VEGF ELISA

Urinary vascular endothelial growth factor was measured by a commercially available ELISA (R&D Systems, Minneapolis, MN). Briefly, 50 μl of urine from a 24-h collection, were added to assay diluent in a 96-well plate for 2 h at room temperature. After washes, VEGF conjugate was added to each well, incubated for 1 h, and then washed four times. The color was developed with substrate solution for 30 min and absorbance read at 450 nm with a correction at 540 nm. All values are expressed as picograms per millimole of creatinine determined by Alfred Hospital Biochemistry autoanalyzer (Alfred Hospital, Melbourne, Australia).

Isolation of skin collagen and analysis of AGEs

Rat skin collagen was prepared as described previously (27). In brief, insoluble collagen was isolated from 1.5-cm^2 pieces of skin after removal of adventitious tissue with a razor blade and subsequent sequential extractions with 1.0 mol/liter NaCl, 0.5 M acetic acid, and delipidation with chloroform-methanol (1:2). The collagen was then lyophilized and stored at −70 C until analysis of AGE/advanced lipoxidation end product content.

CML and pentosidine were quantified in acid hydrolysates of borohydride reduced protein as described previously (27). CML was measured by selected ion monitoring gas chromatography-mass spectrometry and normalized to its parent amino acid lysine. Pentosidine was analyzed by reverse phase-HPLC and normalized to the hydroxyproline content of the collagen.

Superoxide production

Kidneys were rapidly excised, placed in oxygen-saturated Krebs buffer [containing 118 mM NaCl, 4.7 mM KCl, 1.2 mM $MgSO_4.7H_2O$, 1.2 mM KH_2PO_4, 11 mM D-glucose, 0.03 mM EDTA, and 2.5 mM $CaCl_2$ (pH

7.4)] and cut into approximately 1-mm segments. The rate of superoxide anion formation was determined by lucigenin (bis-*N*-methylacridinium nitrate; Sigma). Briefly, 100 μl of substrate [either nicotinamide adenine dinucleotide reduced or nicotinamide adenine dinucleotide phosphate reduced (NADPH), 125 μM] and 30 μM diphenylene iodinium (NADPH-oxidase inhibitor) or 100 μM rotenone (mitochondrial complex I inhibitor) were added to fresh tissue slices (in triplicate). In preliminary studies, the nitric oxide inhibitor L-N^G-nitroarginine was also used; however, this provided no inhibition of superoxide production. The plate was warmed in the luminometer for 60 min at 37 C before the addition of 3.8 μM lucigenin. Chemiluminescence was monitored every 6 min for 60 min, and the integral over this period was expressed as relative light units. Results were normalized to 10 mg dry tissue weight.

Superoxide dismutase activity

The activity of both manganese superoxide dismutase (MnSOD) and copper zinc superoxide dismutase were measured by a commercial activity assay (Cayman Chemical Co., Ann Arbor, MI) according to the manufacturer's instructions. Briefly, 10 μl of mitochondrial or cytosolic isolate or standard in duplicate was added to 200 μl of radical detector. The reaction was initiated by 20 μl xanthine oxidase, incubated for 20 min at room temperature, and the superoxide dismutase activity was measured at 450 nm. Enzymatic activity was expressed as units or milliunits per milligrams of total protein.

Glutathione peroxidase activity

Glutathione peroxidase activity was assessed by an assay kit (Cayman) according to the manufacturer's instructions. Assay buffer (100 μl), 50 μl of cosubstrate mixture (containing NADPH, glutathione, and glutathione reductase), and 20 μl of sample or positive control was added in triplicate 96-well plate. The reaction was initiated by adding 20 μl cumene hydroperoxide, and the absorbance was read once every minute at 340 nm over 5 min.

Hydrogen peroxide production

Hydrogen peroxide generation was measured using a commercial kit (Molecular Probes, Eugene, OR) following the manufacturer's instructions and as described by Mohanty *et al.* (28). Mitochondrial extracts were centrifuged for 2 min at 10,000 × *g*, and pellets were resuspended in Krebs-Ringer phosphate glucose buffer [145 mM NaCl, 5.7 mM sodium phosphate, 4.86 mM KCl, 0.54 mM CaCl$_2$, 1.22 mM MgSO$_4$, 5.5 mM glucose (pH 7.35)]. Twenty microliters of mitochondrial or cytosolic isolate, standard, and blanks were assayed in triplicate in black 96-well plates (Nunc) after addition of prewarmed (37 C) working solution containing 100 μM amplex red reagent and 0.2 U/ml horseradish peroxidase. Fluorescence intensity was measured on a fluorescence microplate reader (Fmax; Molecular Devices, Sunnyvale, CA) over 120 min at excitation 544/Em 590 nm at 37 C.

Nitrotyrosine ELISA

Nitrotyrosine was measured in neat duplicates of both mitochondrial and cytosolic extracts using a sandwich ELISA from Oxis Research (Portland, OR) according to the manufacturer's instructions. The assay uses a mouse monoclonal antibody to capture antigen and a biotin-labeled goat polyclonal anti-nitrotyrosine antibody for detection. The absorbance was determined at a wavelength of 450 nm.

Measurement of NF-κB activity

Nuclear extracts were prepared from the renal cortical pellets above as previously described (11). Nuclear NF-κB activity was measured in duplicate using a NF-κB p65 transcription factor assay kit (TransAM; Active Motif; Carlsbad, CA). Briefly, 10 μg of each sample were incubated with the immobilized oligonucleotide in a 96-well plate. Active NF-κB bound to the oligonucleotide was detected using a specific antibody to the nuclear localization signal region of p65, with bound primary antibody detected with a secondary antibody conjugated to horseradish peroxidase. Absorbances were read at 450 nm with a reference wavelength of 655 nm. Positive controls (Jurkat cell nuclear extract) and mutant and competitor controls were included to monitor the specificity of the assay. A standard curve was also prepared using recombinant NF-κB p65 protein (Active Motif).

PKC activity

An aliquot of the second supernatant from the renal homogenate above was taken and complete protease inhibitors (Roche Diagnostics, Basel, Switzerland) and phosphatase inhibitors added (Sigma). This supernatant was ultracentrifuged at 100,000 × *g* for 1 h at 4 C. The supernatant was discarded and the pellet was resuspended in 20 mM Tris-HCl (pH 7.5), 2 mM EDTA, 10 mM EGTA, 0.25M sucrose, and 1% Triton X-100 and ultracentrifuged at 100,000 × *g* for 1 h at 4 C. This supernatant was retained as the membranous fraction (29). Membranous PKC activity was measured using the StressXpress PKC kinase activity assay kit (EKS-420A; Stressgen Bioreagents Corp., Victoria, British Columbia, Canada). This assay is a solid-phase ELISA that uses a specific synthetic peptide as a substrate for PKC and a polyclonal antibody that recognizes the phosphorylated form of the substrate. Samples were assayed in triplicate and kinase activity determined.

RT-PCR

Three micrograms of total RNA extracted from each kidney cortex were used to synthesize cDNA with the Superscript first-strand synthesis system for RT-PCR (Life Technologies, Inc., Grand Island, NY): AGE-R (AGE receptor)-1 probe, 5′-3′-6-FAM ATCAACGTGGAGAC-CAT, forward primer, 5′-3′-GGGAGTTCCTCTATGACAACCTTATC, reverse primer, 5′-3′-CACCGCCGTCGATGAAG; INT-RAGE probe, 5′-3′-6-FAM, ATCCCAATTCAACCTC, forward primer, 5′-3′-AGAC-GAGCTCCCCCACTCTAC, reverse primer, 5′-3′-GGGCTCTGGTTG-GAGAAGAAA; ABS RAGE probe, 5′-3′-6-FAM TGGTCAGAACATC-ACAGC, forward primer, 5′-3′-CTGGGTACTGGTTCTTGCTCTGT; reverse primer, 5′-3′-CTAGCTTCTGGGTTGGCTTCTTAG; Ang II type 1 (AT1) receptor probe, 5′-3′-6-FAM CTCGCCTTCGCCGCA, forward primer, 5′-3′-CCATCGTCCACCCAATGAAG, reverse primer, 5′-3′-GTGACTTTGGCCACCAGCAT; angiotensinogen probe, 5′-3′-6-FAM CCAACTTCATGGGTTTC, forward primer, 5′-3′-GCCCAGGTCGC-GATGAT, reverse primer, 5′-3′-TTGCCTCACTCAGCATCTTGTACA; renin probe, 5′-3′-6-FAM ATCAGCAAGGCCGGC, forward primer, 5′-3′-AACATTACCAGGGCAACTTTCACT, reverse primer, 5′-3′-AC-CCCCTTCATGGTGATCTG. Gene expression for each of the sequences identified above was analyzed by real-time quantitative RT-PCR performed with the TaqMan system based on real-time detection of accumulated fluorescence (ABI Prism 7700; PerkinElmer) as described previously (30). Each sample was tested in triplicate. Results were expressed relative to control kidneys, which were arbitrarily assigned a value of 1. INT-RAGE refers to probes and primers to the intracellular portion of RAGE. ABS-RAGE refers to probes and primers to the extracellular active binding site of RAGE.

Statistical analysis

Results are expressed as mean ± SD unless otherwise specified. Data for albuminuria were not normally distributed and therefore analyzed after logarithmic transformation. Analyses were performed by ANOVA followed by *post hoc* analysis using Tukey's least significant difference method, correcting for multiple comparisons. A value for $P < 0.05$ was considered to be statistically significant.

Results

Physiological parameters

All diabetic rodents demonstrated a significant elevation of blood glucose and glycated hemoglobin, which was unaffected by any treatment (Table 1). The kidney to body weight ratio was increased in diabetic rats and was not altered by any treatment. Measurement of renal function revealed a 4-fold increase in albuminuria with diabetes, which was essentially normalized in both the DRam and DRamAlt treatment groups. Intervention from 16 to 32 wk with alage-

TABLE 1. Physiological and structural parameters of rodents at 32 wk

	Control			Diabetic			
	Untreated	Ram	RamAlt	Untreated	Ram	RamAlt	Alt
Plasma glucose (mmol/liter)	6.9 ± 0.9	6.7 ± 0.7	6.4 ± 0.5	33.24 ± 2.8[a]	33.14 ± 3.5[a]	33.23 ± 3.1[a]	32.71 ± 4.1[a]
GHb (%)	5.6 ± 0.6	4.9 ± 0.6	5.2 ± 0.7	18.1 ± 2.5[a]	19.0 ± 2.7[a]	18.2 ± 1.7[a]	15.6 ± 2.6[a]
KW to BW ratio × 10³	5.33 ± 0.57	5.47 ± 0.33	5.49 ± 0.68	10.85 ± 1.51[a]	11.29 ± 1.10[a]	11.33 ± 1.39[a]	11.26 ± 1.52[a]
Albuminuria (mg per 24 h)	17.2 ± 12.5	19.8 ± 15.8	12.0 ± 3.8	92.2 ± 65.5[a]	13.9 ± 7.1[b]	18.4 ± 11.4[b]	56.1 ± 28.1[c]
SBP (mm Hg)	114 ± 8	112 ± 8	106 ± 10	134 ± 13[a]	122 ± 8[b]	122 ± 6[b]	127 ± 8[a]
GFR (ml/min·kg)	6.6 ± 1.1	7.0 ± 0.6	7.4 ± 1.3	11.2 ± 1.4[a]	12.0 ± 1.7[a]	11.1 ± 1.5[a]	12.3 ± 1.3[a]

All data are mean ± SD. GFR, Glomerular filtration rate; GHb, glycated hemoglobin; SBP, systolic blood pressure; Ram, ramipril; Alt, alagebrium; KW, kidney weight; BW, body weight.
[a] $P < 0.001$ *vs.* control untreated group.
[b] $P < 0.01$ *vs.* diabetic untreated group.
[c] $P < 0.05$ *vs.* diabetic untreated group.

brium (DAlt) attenuated albuminuria by 40% (Table 1). The glomerular filtration rate markedly increased with diabetes and was not influenced by any treatment.

The RAS

Serum concentrations of Ang II were significantly reduced with diabetes (Fig. 1A). This was only restored to control levels within the combination therapy group (DRamAlt, Fig. 1A). There was a trend toward an increase in the gene expression of renin in renal cortex from diabetic rodents; however, this was not significant ($P = 0.25$; Table 2). Renal angiotensinogen gene expression trended toward a significant decrease, although this was also found not to be significant ($P = 0.19$; Table 2). The AT1 receptor demonstrated a significant reduction in renal gene expression with diabetes, which was not altered with any treatment (Table 2).

Serum CML and renal AGE receptors

An approximately 70% increase in the serum concentration of CML was identified in diabetic rats (Fig. 1B). This was attenuated by all treatments. Skin pentosidine content (C, 1.022 ± 0.371 *vs.* D, 1.411 ± 0.119 μg/g hydroxyproline; $P < 0.01$) was increased in diabetic rodents compared with the control group. No improvement in this AGE was seen with any treatment. Skin CML concentrations were also elevated by diabetes compared with those in skin from control rats (C, 0.043 ± 0.005 *vs.* D, 0.072 ± 0.013 mmol/mol lysine; $P < 0.01$), but again no improvement was seen in any treatment group.

Diabetes induced a 50% reduction in the renal cortical gene expression of ABS-RAGE (which identifies both soluble and full-length RAGE isoforms). This remained unchanged in each of the treatment groups, although there was a trend toward a further decrease in those groups treated with ramipril (Table 2). INT-RAGE, which recognizes the gene expression of both full-length and N-RAGE, remained unaltered in the renal cortex of diabetic rodents (Table 2). The renal gene expression of the AGE clearance receptor AGE-R1, was significantly decreased in diabetic rodents and was restored to control values by alagebrium (DAlt) and the combination of alagebrium and ramipril (DRamAlt, Table 2) but not by ramipril monotherapy. AGE-R3 renal gene expression remained unchanged with diabetes by 32 wk (C, 1.12 ± 0.54 *vs.* D, 1.20 ± 0.43 AU; $P = 0.74$).
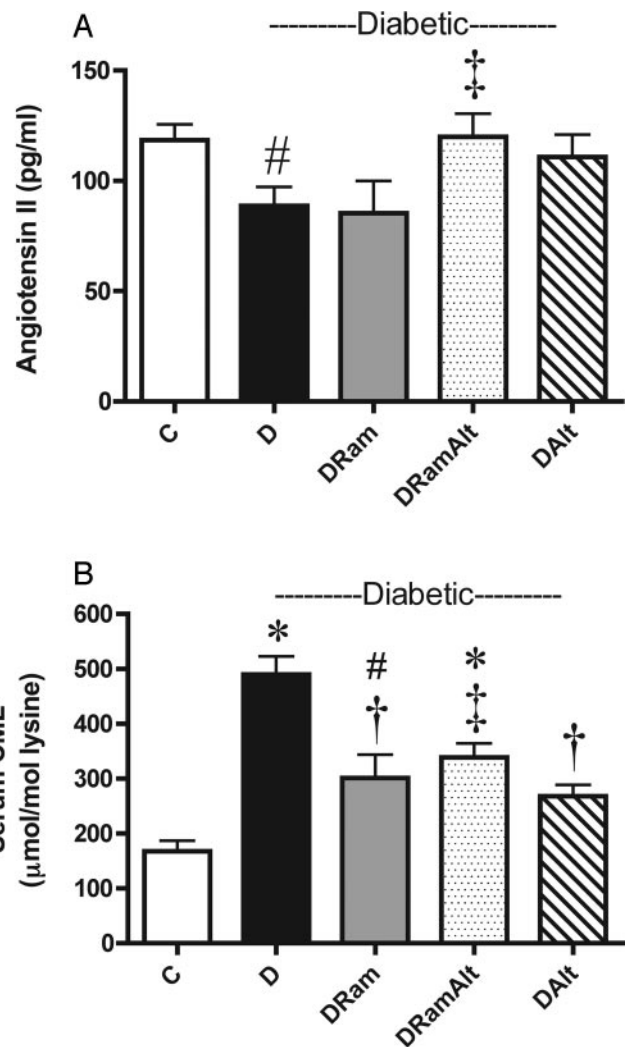
FIG. 1. A, Plasma Ang II concentrations. B, Circulating serum carboxymethyllysine at 32 wk. *, $P < 0.001$ *vs.* control untreated group; †, $P < 0.01$ *vs.* diabetic untreated group; ‡, $P < 0.05$ *vs.* diabetic untreated group; #, $P < 0.05$ *vs.* control untreated group. C, Control; D, diabetic.

Mitochondrial parameters

Renal mitochondrial superoxide production was increased in untreated diabetic rodents (Fig. 2A). This was ameliorated by treatment with alagebrium only (Fig. 2A).

TABLE 2. Gene expression of renal cortical parameters

| Fold induction (arbitrary units)	Control	Diabetic			
	Untreated	Untreated	Ram	RamAlt	Alt
Renin	1.04 ± 0.28	1.68 ± 1.48	1.45 ± 0.09	2.19 ± 1.01	0.71 ± 0.25
Angiotensinogen	1.07 ± 0.43	0.82 ± 0.29	0.67 ± 0.34	0.91 ± 0.41	1.12 ± 0.64
AT1 receptor	1.47 ± 0.62	0.69 ± 0.37^a	0.46 ± 0.19^a	0.34 ± 0.12^a	0.50 ± 0.30^a
ABS-RAGE	1.05 ± 0.37	0.50 ± 0.22^a	0.23 ± 0.19^a	0.73 ± 0.57	$0.18 \pm 0.14^{a,b}$
INT-RAGE	1.02 ± 0.19	1.21 ± 0.36	1.47 ± 0.25	2.01 ± 0.62^b	1.79 ± 0.45^b
AGE-R1	1.08 ± 0.49	0.81 ± 0.11^a	0.89 ± 0.45	1.56 ± 0.70^b	1.09 ± 0.39^b

INT-RAGE, Probes and primers to the intracellular portion of RAGE; ABS-RAGE, probes and primers to the extracellular active binding site of RAGE.

[a] $P < 0.05$ *vs.* control untreated group.
[b] $P < 0.01$ *vs.* diabetic untreated group.

By contrast, renal MnSOD antioxidant activity was significantly reduced with diabetes and was only restored to control values by either alagebrium (DAlt) alone or by combination therapy (DRamAlt, Fig. 2B). No effect of ramipril monotherapy was seen on either mitochondrial superoxide or MnSOD. Diabetes induced a significant elevation in mitochondrial nitrotyrosine, indicative of en-

hanced peroxynitrite formation (Fig. 2C). Each treatment, however, appeared to further elevate nitrotyrosine levels, with only the DAlt group reaching statistical significance (Fig. 2C). Mitochondrial CML concentrations were also increased in kidneys from diabetic rodents (Fig. 2D). Again, all treatments showed a further increase in the CML content of renal mitochondria (Fig. 2D).
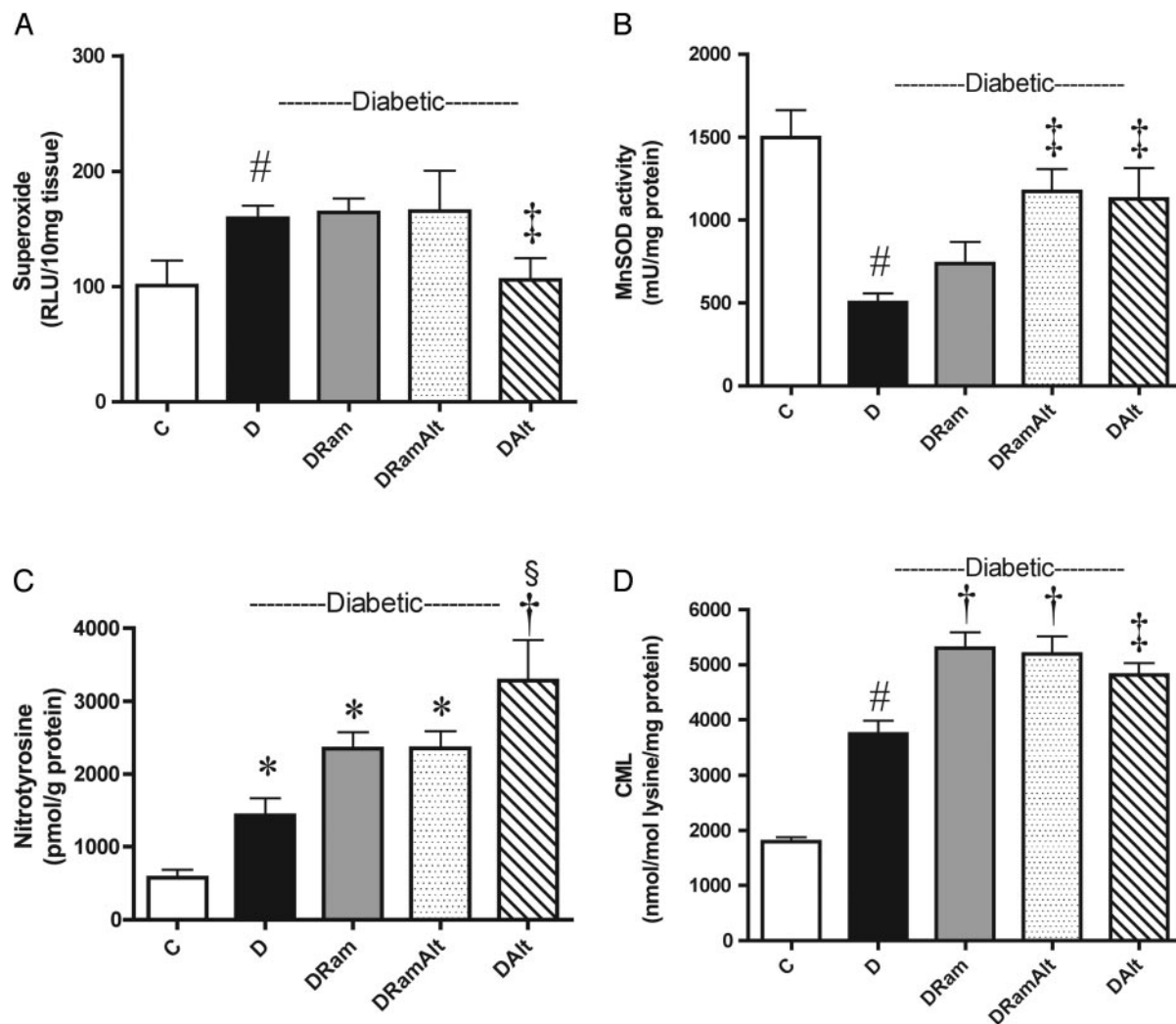
FIG. 2. Renal mitochondrial treatment effects. A, Superoxide generation. B, Manganese containing superoxide dismutase activity. C, Nitrotyrosine. D, Carboxymethyllysine. *, $P < 0.05$ *vs.* control untreated group; †, $P < 0.01$ *vs.* diabetic untreated group; ‡, $P < 0.05$ *vs.* diabetic untreated group; #, $P < 0.01$ *vs.* control untreated group; §, $P < 0.001$ *vs.* control untreated group. C, Control; D, diabetic.

Cytosolic parameters

Renal cytosolic generation of superoxide was increased in diabetic rats (Fig. 3A). Each of the treatments were effective in attenuating this diabetes associated increase in superoxide production (Fig. 3A). Hydrogen peroxide generation was decreased in renal tissues of diabetic rodents; however, there was no change identified in any of the treatment groups (Fig. 3B). The activity of the antioxidant glutathione peroxidase was elevated by diabetes but remained unaltered by any treatment (Fig. 3C). There was no change in renal cytosolic nitrotyrosine content with diabetes or with any treatment (C, 2284 ± 590 *vs.* D, 2206 ± 584 pmol/g protein; $P = 0.79$). Cytosolic CML content was significantly increased in the renal cortical cytosolic extract from diabetic rats and was unaltered with therapy (Fig. 3D).

Renal NF-κB and PKC activation

The nuclear content of the activated p65 subunit of NF-κB was significantly increased in renal cortex from diabetic rodents (Fig. 4A). However, activated p65 remained unchanged by any treatment. Renal cortical gene expression of both the p65 subunit of NF-κB (C, 1.04 ± 0.34 *vs.* D, 1.02 ± 0.46 AU; $P = 0.83$) and its inhibitor, inhibitor-κB-α (C, 1.08 ± 0.41 *vs.* D, 0.98 ± 0.23 AU; $P = 0.54$) were unaltered after 32 wk of diabetes or with any therapy. The membrane content of active PKC showed a significant increase with diabetes (Fig. 4B). All the treatments attenuated this increase in PKC activity to control levels.

Urinary VEGF excretion

Urinary excretion of VEGF was significantly elevated with diabetes (Fig. 4C). This was attenuated by both ramipril and by ramipril in combination with alagebrium. There was a trend toward a reduction in urinary VEGF with alagebrium alone; however, this did not reach statistical significance ($P = 0.09$; Fig. 4C).

Discussion

The present study has shown the efficacy of blocking two individual pathways, namely the RAS and advanced glycation, which appear to contribute to renal damage in diabetes. The rationale of the study involved assessment of the AGE cross-link breaker as adjunct therapy because ACE inhibition is already accepted as a routine treatment approach for diabetic renal disease. These experiments did not demonstrate
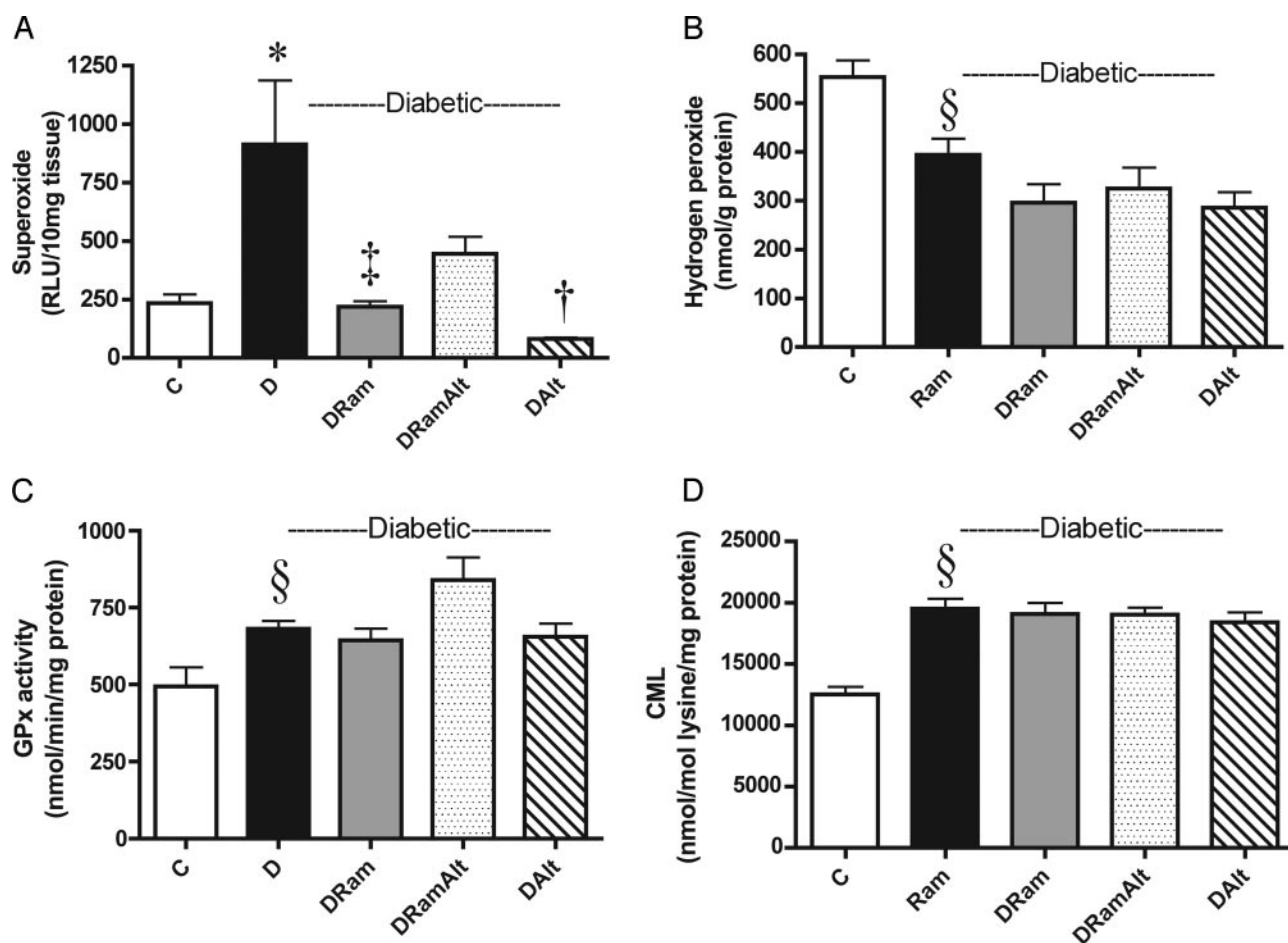
FIG. 3. Renal cortical cytosolic treatment effects. A, Superoxide generation. B, Hydrogen peroxide generation. C, Glutathione peroxidase activity. D, Carboxymethyllysine. Nitrotyrosine and copper-zinc containing superoxide dismutase activity were not found to be different between control and diabetic rodents ($P = 0.8182$ for copper zinc superoxide dismutase). *, $P < 0.001$ *vs.* control untreated group; †, $P < 0.01$ *vs.* diabetic untreated group; ‡, $P < 0.05$ *vs.* diabetic untreated group; §, $P < 0.05$ *vs.* control untreated group. C, Control; D, diabetic.
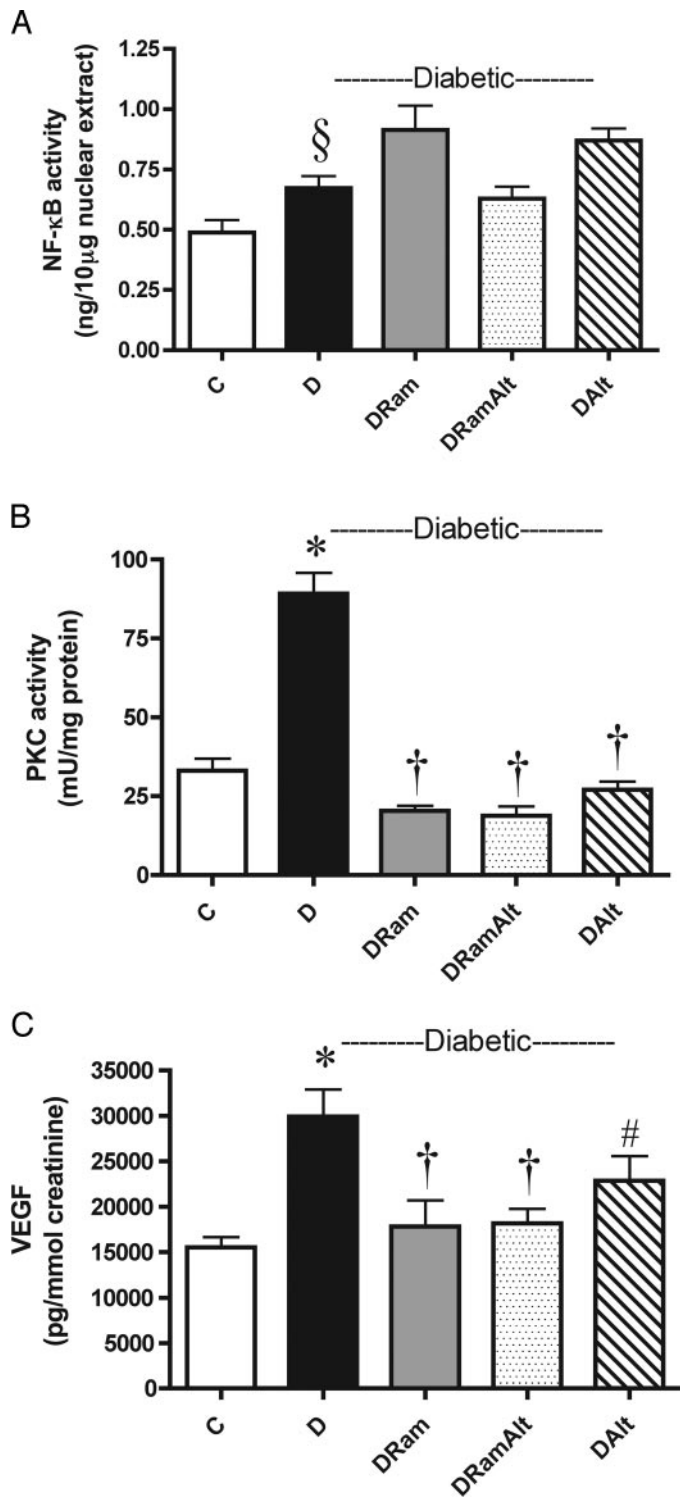
FIG. 4. Renal cortical measures of NF-κB and PKC. A, NF-κB p65 activation. B, Membrane PKC activity. C, Urinary vascular endothelial growth factor excretion. *, $P < 0.001$ *vs.* control untreated group; †, $P < 0.01$ *vs.* diabetic untreated group; §, $P < 0.05$ *vs.* control untreated group. C, Control; D, diabetic.

a clear-cut benefit of combination therapy. Specifically, an additional renoprotective role of adding blockade of advanced glycation to established ACEi in diabetic rodents was

not readily observed in this normotensive model of nephropathy, although for certain downstream parameters implicated in the progression of diabetic renal disease, there were distinct benefits seen with blockade of advanced glycation.

Previously ACE inhibitors (21, 22) and alagebrium (31) have demonstrated a capacity to reduce both the renal and circulating accumulation of fluorescent low molecular weight advanced glycation end products in diabetic nephropathy. This was not, however, demonstrated within the present study, in which a lack of effect of ACEi, ramipril, or alagebrium alone and their combination in reducing renal mitochondrial and cytosolic accumulation of the AGE, CML was identified. Furthermore, this lack of an effect within certain renal compartments was also observed when assessing skin collagen-associated AGEs, CML and pentosidine. The efficacy of reducing skin collagen-associated CML and pentosidine with alagebrium has been previously demonstrated by our group in a model of diabetes-accelerated atherosclerosis (32). However, because in that study alagebrium also improved the lipid profile, which is markedly abnormal due to the apolipoprotein E deficiency in those mice, it is likely that a major source of skin collagen AGEs in that setting was from fatty acids rather than reducing sugars. This is supported by a recent study by Peppa *et al.* (33), in which there was improvement of skin CML by treatment with alagebrium in db/db mice. This link between lipids and tissue AGE levels has also been previously shown in diabetic rodents treated with pyridoxamine in a model in which reduced lipid levels were also observed with treatment (34).

The absence of improvements in the intracellular AGE, CML, either within renal mitochondria or the cytosol, supports previous studies demonstrating AGE synthesis *de novo* inside the cell, most likely from glucose, other reducing sugars derived from glycolysis and the tricarboxylic acid cycle (35, 36). This suggests that alagebrium, considered to be a cross-link breaker, and ramipril may not pharmacologically inhibit renal intracellular AGE formation. In addition, it appears that the intracellular formation of CML is not dependent on or facilitated by superoxide generation in this model, as has been previously suggested (37), because alagebrium was extremely effective at reducing the genesis of superoxide in both mitochondria and the cytosol. Furthermore, the combination with ramipril attenuated superoxide production in the cytosol, although this is likely to be due to alagebrium *per se*, because alagebrium as monotherapy conferred a similar effect. These findings also raise the possibility that intracellular superoxide generation may be occurring as a result of an external AGE-dependent stimulus such as the interaction between circulating AGEs and the RAGE receptor. This concept is also supported by the amelioration of serum AGE levels with alagebrium alone, as seen in a recent study (33) or in combination with ramipril. This generation of intracellular superoxide via the AGE-RAGE interaction has been demonstrated previously (38, 39). Therefore, the improvement of circulating rather than tissue AGE (CML) levels was more closely associated with reduced albuminuria. The diabetes-induced increase in renal NF-κB activation provides further circumstantial evidence for activation of RAGE by ligands such as AGEs because this ligand receptor interaction has previously been shown to be a potent activator of NF-κB

(40) and may play a more direct role in early end organ injury than intracellularly generated AGEs.

It remains to be determined, however, as to why alagebrium is a more efficient blocker of superoxide formation both from the respiratory chain and via NADPH oxidase. Within renal mitochondria from diabetic rodents, the decline in the activity of the antioxidant enzyme, MnSOD could explain the excess of mitochondrial superoxide evident in this experimental model. This superoxide appears to be redirected to combine with nitric oxide to produce the peroxynitrite radical, $ONOO^-$, and this is supported by the increase in mitochondrial nitrotyrosine seen with diabetes in this study. The restoration of MnSOD activity to control levels in both the alagebrium and combination therapy groups provides further evidence for this pathway because this maximizes the dismutation of superoxide to hydrogen peroxide rather than leaving excess superoxide available for combination with nitric oxide. It is puzzling, however, that these treatment benefits did not translate into decreases in mitochondrial nitrotyrosine, and this warrants further investigation.

Clearly defined in the present study are the benefits of treatment in diabetic nephropathy on cytosolic superoxide production, which also translated into less accumulation of hydrogen peroxide. As previously mentioned, it is likely that at least part of this effect is extracellularly mediated via binding of circulating AGEs to receptors, most likely, RAGE. Other studies have demonstrated that activation of RAGE leads to the generation of cytosolic superoxide via NADPH oxidase (39). Indeed, we have previously demonstrated a significant increase in renal RAGE in this model at 32 wk of diabetes (31). This is also reflected by the diabetes-dependent decline in the expression of AGE-R1, postulated to be protective in diabetic nephropathy (41). Indeed, AGE-R1 has recently been shown to inversely modulate the expression of RAGE in renal cells (42). Renal AGE-R1 expression in the present study was normalized by both alagebrium and its combination with ramipril, which further supports an AGE-RAGE interaction as a possible pathway contributing to superoxide generation. The ability of ramipril alone to improve renal cytosolic superoxide may be due to its capacity to increase circulating soluble RAGE concentrations (43), which acts as an antagonist by directly competing with cellular (full length) RAGE for circulating AGEs. Such an effect may provide an explanation for the observed decrease in circulating AGEs by ramipril in the absence of effects on cellular superoxide.

Alagebrium has been shown to be a specific inhibitor of PKCα activation by our group (44). Furthermore, it was shown that *in vivo* administration of various inhibitors of advanced glycation, including alagebrium, reduce PKCβI expression. Within the present study, an increase in membranous PKC activity was observed in diabetic renal cortex. Thus, it is not totally surprising that alagebrium and the combination therapy, which included alagebrium, restored PKC activity to control levels. The effect of ramipril alone in decreasing PKC activity may relate to its ability to reduce Ang II formation because Ang II *per se* has been demonstrated to activate PKC (9, 45).

There was a reduction in plasma Ang II in diabetic animals

consistent with previous reports of reduced levels in the systemic circulation of various components of the RAS including not only Ang II but also plasma renin activity (46). The restoration of plasma Ang II with alagebrium remains to be explained. If this represents an indirect effect via beneficial actions of this agent on the diabetic kidney or is related to the ability of alagebrium to modulate second messengers such as PKCα (44) remains to be directly tested.

Renal Ang II and specifically AT1 receptor subtype expression has been previously described to in general be decreased in experimental diabetes (47–49). However, this reduction in Ang II receptor expression does not indicate that the AT1 receptor is not functionally as active in the diabetic context because these techniques do not address postreceptor signaling events. Indeed, it has been demonstrated that there is an increase in sensitivity to Ang II in the diabetic kidney, both in experimental and clinical studies (50, 51), and this has been postulated to partly explain the renoprotective effects that have been amply demonstrated in both experimental and human diabetes.

The significant improvements in urinary albumin excretion in groups treated with ACEi (22) and alagebrium (31) have been previously described. Further improvement of albuminuria with combination therapy may not have been possible due to maximal normalization via monotherapy with ramipril. In addition to these beneficial functional renal effects, diabetes-induced increases in urinary VEGF excretion were also abrogated with ramipril therapy, although the alagebrium monotherapy group did not appear to be as effective as the treatment groups that included the ACE inhibitor. This, however, may have been due to the fact that monotherapy with alagebrium was administered only from wk 16 of the study and not from the onset of diabetes as was instituted for ramipril treatments. The link between VEGF and albuminuria has been previously demonstrated more directly with previous studies reporting that a neutralizing antibody to VEGF significantly improved albuminuria in various animal models of diabetes (18).

The present study has identified a complex series of interactions linking cytosolic and mitochondrial oxidative stress, the RAS, PKC, and advanced glycation in the development of diabetic nephropathy. The various pathways such as advanced glycation and the RAS appear to share common mediators which may ultimately prove to be more effective as targets for new renoprotective therapies in diabetes.

References

1. **Brownlee M** 2001 Biochemistry and molecular cell biology of diabetic complications. Nature 414:813–820
2. **Cooper ME** 2001 Interaction of metabolic and haemodynamic factors in mediating experimental diabetic nephropathy. Diabetologia 44:1957–1972
3. **Lewis EJ, Hunsicker LG, Bain RP, Rohde RD** 1993 The effect of angiotensin-converting-enzyme inhibition on diabetic nephropathy. The Collaborative Study Group. N Engl J Med 329:1456–1462
4. **Brenner BM, Cooper ME, de Zeeuw D, Keane WF, Mitch WE, Parving HH, Remuzzi G, Snapinn SM, Zhang Z, Shahinfar S** 2001 Effects of losartan on renal and cardiovascular outcomes in patients with type 2 diabetes and nephropathy. N Engl J Med 345:861–869
5. **Jerums G, Allen TJ, Campbell DJ, Cooper ME, Gilbert RE, Hammond JJ, Raffaele J, Tsalamandris C** 2001 Long-term comparison between perindopril and nifedipine in normotensive patients with type 1 diabetes and microalbuminuria. Am J Kidney Dis 37:890–899
6. **Nishikawa T, Edelstein D, Du XL, Yamagishi S, Matsumura T, Kaneda Y, Yorek MA, Beebe D, Oates PJ, Hammes HP, Giardino I, Brownlee M** 2000 Normalizing mitochondrial superoxide production blocks three pathways of hyperglycaemic damage. Nature 404:787–790
7. **Scivittaro V, Ganz MB, Weiss MF** 2000 AGEs induce oxidative stress and activate protein kinase C-β(II) in neonatal mesangial cells. Am J Physiol Renal Physiol 278:F676–F683
8. **Baynes JW** 1991 Role of oxidative stress in development of complications in diabetes. Diabetes 40:405–412
9. **Osicka TM, Yu YX, Panagiotopoulos S, Clavant SP, Kiriazis Z, Pike RN, Pratt LM, Russo LM, Kemp BE, Comper WD, Jerums G** 2000 Prevention of albuminuria by aminoguanidine or ramipril in streptozotocin-induced diabetic rats is associated with the normalization of glomerular protein kinase C. Diabetes 49:87–93
10. **Ruiz-Ortega M, Lorenzo O, Ruperez M, Konig S, Wittig B, Egido J** 2000 Angiotensin II activates nuclear transcription factor κB through AT(1) and AT(2) in vascular smooth muscle cells: molecular mechanisms. Circ Res 86:1266–1272
11. **Lee FT, Cao Z, Long DM, Panagiotopoulos S, Jerums G, Cooper ME, Forbes JM** 2004 Interactions between angiotensin II and NFκB-dependent pathways in modulating macrophage infiltration in experimental diabetic nephropathy. J Am Soc Nephrol 15:2139–2151
12. **Brownlee M, Vlassara H, Kooney A, Ulrich P, Cerami A** 1986 Aminoguanidine prevents diabetes-induced arterial wall protein cross-linking. Science 232:1629–1632
13. **Soulis T, Thallas V, Youssef S, Gilbert RE, McWilliam B, Murray-McIntosh RP, Cooper ME** 1997 Advanced glycation end products and the receptor for advanced glycated end products co-localise in organs susceptible to diabetic microvascular injury: immunohistochemical studies. Diabetologia 40:619–628
14. **Wendt TM, Tanji N, Guo J, Kislinger TR, Qu W, Lu Y, Bucciarelli LG, Rong LL, Moser B, Markowitz GS, Stein G, Bierhaus A, Liliensiek B, Arnold B, Nawroth PP, Stern DM, D'Agati VD, Schmidt AM** 2003 RAGE drives the development of glomerulosclerosis and implicates podocyte activation in the pathogenesis of diabetic nephropathy. Am J Pathol 162:1123–1137
15. **Morcos M, Sayed AA, Bierhaus A, Yard B, Waldherr R, Merz W, Kloeting I, Schleicher E, Mentz S, Abd el Baki RF, Tritschler H, Kasper M, Schwenger V, Hamann A, Dugi KA, Schmidt AM, Stern D, Ziegler R, Haering HU, Andrassy M, van der Woude F, Nawroth PP** 2002 Activation of tubular epithelial cells in diabetic nephropathy. Diabetes 51:3532–3544
16. **De Vriese AS, Tilton RG, Stephan CC, Lameire NH** 2001 Vascular endothelial growth factor is essential for hyperglycemia-induced structural and functional alterations of the peritoneal membrane. J Am Soc Nephrol 12:1734–1741
17. **Flyvbjerg A, Dagnaes-Hansen F, De Vriese AS, Schrijvers BF, Tilton RG, Rasch R** 2002 Amelioration of long-term renal changes in obese type 2 diabetic mice by a neutralizing vascular endothelial growth factor antibody. Diabetes 51:3090–3094
18. **Schrijvers BF, Flyvbjerg A, Tilton RG, Lameire NH, De Vriese AS** 2006 A neutralizing VEGF antibody prevents glomerular hypertrophy in a model of obese type 2 diabetes, the Zucker diabetic fatty rat. Nephrol Dial Transplant 21:324–329
19. **Bierhaus A, Humpert PM, Morcos M, Wendt T, Chavakis T, Arnold B, Stern DM, Nawroth PP** 2005 Understanding RAGE, the receptor for advanced glycation end products. J Mol Med 83:876–886
20. **Thomas MC, Tikellis C, Burns WM, Bialkowski K, Cao Z, Coughlan MT, Jandeleit-Dahm K, Cooper ME, Forbes JM** 2005 Interactions between renin angiotensin system and advanced glycation in the kidney. J Am Soc Nephrol 16:2976–2984
21. **Miyata T, van Ypersele de Strihou C, Ueda Y, Ichimori K, Inagi R, Onogi H, Ishikawa N, Nangaku M, Kurokawa K** 2002 Angiotensin II receptor antagonists and angiotensin-converting enzyme inhibitors lower *in vitro* the formation of advanced glycation end products: biochemical mechanisms. J Am Soc Nephrol 13:2478–2487
22. **Forbes JM, Cooper ME, Thallas V, Burns WC, Thomas MC, Brammar GC, Lee F, Grant SL, Burrell LA, Jerums G, Osicka TM** 2002 Reduction of the accumulation of advanced glycation end products by ACE inhibition in experimental diabetic nephropathy. Diabetes 51:3274–3282
23. **Bunag RD** 1973 Validation in awake rats of a tail-cuff method for measuring systolic pressure. J Appl Physiol 34:279–282
24. **O'Brien RC, Allen TJ, Cooper ME, Bach L, Jerums G** 1988 Glomerular filtration rate in early experimental diabetes. J Diabetes Complications 2:8–11
25. **Cefalu WT, Wang ZQ, Bell-Farrow A, Kiger FD, Izlar C** 1994 Glycohemoglobin measured by automated affinity HPLC correlates with both short-term and long-term antecedent glycemia. Clin Chem 40:1317–1321
26. **Forbes JM, Soulis T, Thallas V, Panagiotopoulos S, Long DM, Vasan S, Wagle D, Jerums G, Cooper ME** 2001 Renoprotective effects of a novel inhibitor of advanced glycation. Diabetologia 44:108–114
27. **Degenhardt TP, Alderson NL, Arrington DD, Beattie RJ, Basgen JM, Steffes MW, Thorpe SR, Baynes JW** 2002 Pyridoxamine inhibits early renal disease and dyslipidemia in the streptozotocin-diabetic rat. Kidney Int 61:939–950
28. **Mohanty JG, Jaffe JS, Schulman ES, Raible DG** 1997 A highly sensitive fluorescent micro-assay of H2O2 release from activated human leukocytes using a dihydroxyphenoxazine derivative. J Immunol Methods 202:133–141
29. **Baines CP, Zhang J, Wang GW, Zheng YT, Xiu JX, Cardwell EM, Bolli R, Ping P** 2002 Mitochondrial PKCε and MAPK form signaling modules in the murine heart: enhanced mitochondrial PKCε-MAPK interactions and differential MAPK activation in PKCε-induced cardioprotection. Circ Res 90:390–397
30. **Forbes JM, Bonnet F, Russo LM, Burns WC, Cao Z, Candido R, Kawachi H, Allen TJ, Cooper ME, Jerums G, Osicka TM** 2002 Modulation of nephrin in the diabetic kidney: association with systemic hypertension and increasing albuminuria. J Hypertens 20:985–992
31. **Forbes JM, Thallas V, Thomas MC, Founds HW, Burns WC, Jerums G, Cooper ME** 2003 The breakdown of preexisting advanced glycation end products is associated with reduced renal fibrosis in experimental diabetes. FASEB J 17:1762–1764
32. **Forbes JM, Yee LT, Thallas V, Lassila M, Candido R, Jandeleit-Dahm KA, Thomas MC, Burns WC, Deemer EK, Thorpe SR, Cooper ME, Allen TJ** 2004 Advanced glycation end product interventions reduce diabetes-accelerated atherosclerosis. Diabetes 53:1813–1823
33. **Peppa M, Brem H, Cai W, Zhang JG, Basgen J, Li Z, Vlassara H, Uribarri J** 2006 Prevention and reversal of diabetic nephropathy in db/db mice treated with alagebrium (ALT-711). Am J Nephrol 26:430–436
34. **Alderson NL, Chachich ME, Youssef NN, Beattie RJ, Nachtigal M, Thorpe SR, Baynes JW** 2003 The AGE inhibitor pyridoxamine inhibits lipemia and development of renal and vascular disease in Zucker obese rats. Kidney Int 63:2123–2133
35. **Shinohara M, Thornalley PJ, Giardino I, Beisswenger P, Thorpe SR, Onorato J, Brownlee M** 1998 Overexpression of glyoxalase-I in bovine endothelial cells inhibits intracellular advanced glycation endproduct formation and prevents hyperglycemia-induced increases in macromolecular endocytosis. J Clin Invest 101:1142–1147
36. **Thornalley PJ, Langborg A, Minhas HS** 1999 Formation of glyoxal, methylglyoxal and 3-deoxyglucosone in the glycation of proteins by glucose. Biochem J 344(Pt 1):109–116
37. **Onorato JM, Jenkins AJ, Thorpe SR, Baynes JW** 2000 Pyridoxamine, an inhibitor of advanced glycation reactions, also inhibits advanced lipoxidation reactions. Mechanism of action of pyridoxamine. J Biol Chem 275:21177–21184
38. **Yan SD, Schmidt AM, Anderson GM, Zhang JH, Brett J, Zou YS, Pinsky D, Stern D** 1994 Enhanced cellular oxidant stress by the interaction of advanced glycation end products with their receptors binding proteins. J Biol Chem 269:9889–9897
39. **Wautier MP, Chappey O, Corda S, Stern DM, Schmidt AM, Wautier JL** 2001 Activation of NADPH oxidase by AGE links oxidant stress to altered gene expression via RAGE. Am J Physiol Endocrinol Metab 280:E685–E694
40. **Bierhaus A, Schiekofer S, Schwaninger M, Andrassy M, Humpert PM, Chen J, Hong M, Luther T, Henle T, Kloting I, Morcos M, Hofmann M, Tritschler H, Weigle B, Kasper M, Smith M, Perry G, Schmidt AM, Stern DM, Haring HU, Schleicher E, Nawroth PP** 2001 Diabetes-associated sustained activation of the transcription factor nuclear factor-κB. Diabetes 50:2792–2808
41. **Liu H, Zhu L, Zheng F, Vlassara H** 2005 Overexpression of AGE-receptor-1 (AGE-R1) in mice prevent AGE accumulation and delays diabetic renal injury. Diabetes 54:A21–A3.
42. **Lu C, He JC, Cai W, Liu H, Zhu L, Vlassara H** 2004 Advanced glycation endproduct (AGE) receptor 1 is a negative regulator of the inflammatory response to AGE in mesangial cells. Proc Natl Acad Sci USA 101:11767–11772
43. **Forbes JM, Thorpe SR, Thallas-Bonke V, Pete J, Thomas MC, Deemer ER, Bassal S, El-Osta A, Long DM, Panagiotopoulos S, Jerums G, Osicka TM, Cooper ME** 2005 Modulation of soluble receptor for advanced glycation end products by angiotensin-converting enzyme-1 inhibition in diabetic nephropathy. J Am Soc Nephrol 16:2363–2372
44. **Thallas-Bonke V, Lindschau C, Rizkalla B, Bach LA, Boner G, Meier M, Haller H, Cooper ME, Forbes JM** 2004 Attenuation of extracellular matrix accumulation in diabetic nephropathy by the advanced glycation end product cross-link breaker ALT-711 via a protein kinase C-α-dependent pathway. Diabetes 53:2921–2930
45. **Nagahama T, Hayashi K, Ozawa Y, Takenaka T, Saruta T** 2000 Role of protein

kinase C in angiotensin II-induced constriction of renal microvessels. Kidney Int 57:215–223

46. **Christlieb AR** 1976 Renin-angiotensin-aldosterone system in diabetes mellitus. Diabetes 25:820–825

47. **Bonnet F, Candido R, Carey RM, Casley D, Russo LM, Osicka TM, Cooper ME, Cao Z** 2002 Renal expression of angiotensin receptors in long-term diabetes and the effects of angiotensin type 1 receptor blockade. J Hypertens 20:1615–1624

48. **Wilkes BM** 1987 Reduced glomerular angiotensin II receptor density in diabetes mellitus in the rat: time course and mechanism. Endocrinology 120:1291–1298

49. **Ballermann BJ, Skorecki KL, Brenner BM** 1984 Reduced glomerular angiotensin II receptor density in early untreated diabetes mellitus in the rat. Am J Physiol 247:F110–F116

50. **Kennefick TM, Oyama TT, Thompson MM, Vora JP, Anderson S** 1996 Enhanced renal sensitivity to angiotensin actions in diabetes mellitus in the rat. Am J Physiol 271:F595–F602

51. **Hollenberg NK, Price DA, Fisher ND, Lansang MC, Perkins B, Gordon MS, Williams GH, Laffel LM** 2003 Glomerular hemodynamics and the renin-angiotensin system in patients with type 1 diabetes mellitus. Kidney Int 63:172–178

Endocrinology is published monthly by The Endocrine Society (http://www.endo-society.org), the foremost professional society serving the endocrine community.